



HAL
open science

Human-subject Evaluation of Shared-Control Approaches for Robotic Telemanipulation

Firas Abi-Farraj, Claudio Pacchierotti, Paolo Robuffo Giordano

► **To cite this version:**

Firas Abi-Farraj, Claudio Pacchierotti, Paolo Robuffo Giordano. Human-subject Evaluation of Shared-Control Approaches for Robotic Telemanipulation. 2017 IEEE/RSJ IROS Workshop Human in-the-loop robotic manipulation: on the influence of the human role, Sep 2017, Vancouver, Canada. hal-01691114

HAL Id: hal-01691114

<https://inria.hal.science/hal-01691114>

Submitted on 23 Jan 2018

HAL is a multi-disciplinary open access archive for the deposit and dissemination of scientific research documents, whether they are published or not. The documents may come from teaching and research institutions in France or abroad, or from public or private research centers.

L'archive ouverte pluridisciplinaire **HAL**, est destinée au dépôt et à la diffusion de documents scientifiques de niveau recherche, publiés ou non, émanant des établissements d'enseignement et de recherche français ou étrangers, des laboratoires publics ou privés.

Human-subject Evaluation of Shared-Control Approaches for Robotic Telemanipulation

Firas Abi-Farraj, Claudio Pacchierotti and Paolo Robuffo Giordano

I. INTRODUCTION

Remote telemanipulation has shown significant advancements over the last years and promising results have been achieved in several robotic tasks [1], [2]. Handling radioactive waste in nuclear decommissioning sites is an important example of such a task where telemanipulation systems are already heavily used. However, currently-employed systems are still extremely primitive, making the handling of these materials prohibitively slow and ineffective. As the estimated cost for the decommissioning and clean-up of nuclear sites keeps rising, it is clear that one would need faster and more effective approaches.

Towards this goal, several recent works have been presented in the context of the European H2020 Robotic Manipulation for Nuclear Sort and Segregation (RoMaNS) project [3], [4]. We present, in this context, the evaluation of a haptic-enabled shared-control architecture for telemanipulation. It was inspired by the work of Abi-Farraj et al. [5], who presented the algorithmic design of the shared-control architecture, but without providing any user evaluation. The experimental setup is shown in Fig. 1. The master system is composed of the Haption Virtuose 6D haptic device, a high performance force feedback device with three active translational DoF and three active rotational DoF. The slave system is composed of a 6-DoF Viper S850 robotic arm carrying a pneumatic parallel gripper. A wooden object is placed on a table in front of the robotic manipulator. An autonomous algorithm is in charge of regulating a subset of the manipulator DoF to help the human operator in grasping the object. At the same time, the human operator steers the robotic end-effector along the remaining null-space directions with respect to the main task using the Virtuose haptic interface.

II. SHARED CONTROL ARCHITECTURE

In our implementation, the autonomous algorithm controls 2 DoF of the robotic manipulator, keeping the gripper always oriented toward the object to grasp. The gripper is therefore constrained to move on the surface of a virtual sphere centered on the object. The human operator is then able to move the gripper across the surface of the sphere and toward/away from the object (i.e., changing the radius of the sphere), controlling the remaining 4 DoF of the robot.

To this end, let s be the variable designating the direction from the gripper to the object $s = {}^G P_O / \| {}^G P_O \| \in \mathbb{S}^2$. The autonomous algorithm drives s to be aligned with the z-axis of the gripper in order to keep the gripper oriented towards the object as described before. The control law governing the

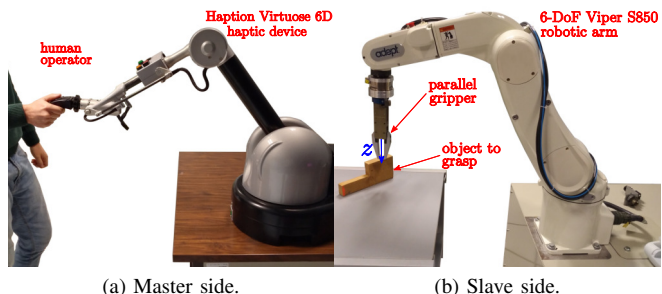


Fig. 1. Experimental setup.

motion of the gripper will then be

$$\mathbf{V}_G = \begin{bmatrix} v_G \\ \omega_G \end{bmatrix} = k_G \mathbf{L}_s^\dagger (\mathbf{Z}_G - \mathbf{s}) + \sum_{i=1}^n \lambda_i \mathbf{n}_i, \quad k_G > 0, \quad (1)$$

where k_G is a control gain, \mathbf{L}_s^\dagger represents the Moore-Penrose pseudo-inverse of the interaction matrix \mathbf{L}_s associated with \mathbf{s} ($\dot{\mathbf{s}} = \mathbf{L}_s \mathbf{V}_G$), \mathbf{Z}_G is the axis associated with the gripper (fig. 1), $\boldsymbol{\lambda} = [\dots \lambda_i \dots] \in \mathbb{R}^4$ indicates the pseudo-velocity commands of the human operator and $\mathbf{N}_B = [\dots \mathbf{n}_i \dots] \in \mathbb{R}^{6 \times 4}$ is a basis spanning the null space of \mathbf{L}_s .

On the master side, the force feedback received by the operator mainly aims at keeping the user away from pre-defined constraints (singularities and joint limits in our scenario), which are described by a cost function H . The corresponding force cues are then defined by

$$\boldsymbol{\tau} = -\mathbf{B}_M \dot{\mathbf{x}}_M - \left(\frac{\partial H(\mathbf{q})}{\partial \mathbf{q}} \right)^T \mathbf{J}_G^{-1}(\mathbf{q}) \mathbf{n}_i, \quad (2)$$

i.e., by projecting the joint motion caused by the i -th null-space direction \mathbf{n}_i onto the negative gradient of $H(\mathbf{q})$. Matrix $\mathbf{J}_G(\mathbf{q}) \in \mathbb{R}^{6 \times 6}$ is the geometric Jacobian of the manipulator. $\mathbf{B}_M \in \mathbb{R}^{4 \times 4}$ is a positive definite matrix indicating the damping factor and \mathbf{x}_M represents the master device's configuration vector.

III. EXPERIMENTAL EVALUATION

A. Experimental conditions, task, and participants

Participants were required to control the motion of the robotic manipulator and gripper to grasp the wooden piece and lift it from the ground.

We considered two different ways of commanding the motion of the robot through the haptic interface

- 1) Position-Velocity (PV): positions of the haptic device are mapped into velocities of the manipulator
- 2) Velocity-Velocity (VV): velocities of the haptic device are mapped into velocities of the manipulator.

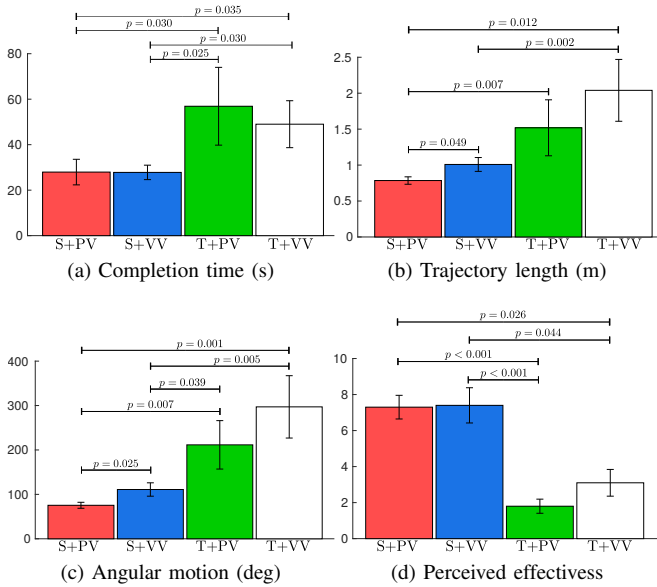


Fig. 2. Experimental evaluation. Mean and 95% confidence interval of (a) completion time, (b) trajectory length, (c) angular motion, and (d) perceived effectiveness of the four feedback conditions are plotted.

Moreover, two different levels of human involvement in the control are considered (shared control vs. teleoperation)

- 1) Shared Control (S): the subject controls only 4 DoF of the manipulator
- 2) Teleoperation (T): the subject controls all 6 DoF of the manipulator.

We end up with four different experimental conditions representing the four possible combinations of the described control and commanding modes: S+PV, S+VV, T+PV and T+VV. The shared-control architectures, employed in conditions S+PV and S+VV, are summarized in Sec. I and described in details in [5]. In T+PV and T+VV conditions, the subject is in *full* control of the manipulator’s 6 DoF.

Ten subjects participated in the study, carrying out 2 repetitions of the grasping task per experimental condition.

B. Results

We recorded (i) the completion time, (ii) the linear trajectory followed by the robotic end-effector, (iii) the angular motion of the robotic end-effector, and (iv) the perceived effectiveness of the different conditions. To compare the different metrics, we ran both two-way and one-way repeated-measures ANOVA tests on the data. All data passed the Shapiro-Wilk normality test.

Figure 2a shows the average task completion time. The two-way ANOVA test revealed a statistically significant change in the task completion time for the human involvement in the control variable (shared control vs. teleoperation, $F(1, 9) = 25.852$, $p = 0.001$). The one-way ANOVA test revealed a statistically significant change in the task completion time across the conditions ($F(3, 27) = 9.312$, $p < 0.001$). Post hoc analysis with Bonferroni adjustments revealed a statistically significant difference between S+V vs. T+V ($p = 0.030$), S+V vs. T+P ($p = 0.035$), S+P vs. T+V ($p = 0.031$), and S+P vs. T+P ($p = 0.025$).

Figure 2b shows the average linear motion covered by the robotic gripper during the task. The two-way ANOVA test revealed a statistically significant change in the trajectory length for both the human involvement in the control ($F(1, 9) = 30.968$, $p < 0.001$) and the motion control type (velocity vs. position, $F(1, 9) = 9.035$, $p = 0.015$) variables. The one-way ANOVA test revealed a statistically significant change in the trajectory length across the conditions ($F(1.929, 17.360) = 14.072$, $p < 0.001$). Post hoc analysis with Bonferroni adjustments revealed a statistically significant difference between S+V vs. S+P ($p = 0.049$), S+V vs. T+V ($p = 0.043$), S+V vs. T+P ($p = 0.002$), and S+P vs. T+P ($p = 0.012$).

Figure 2c shows the average angular motion covered by the robotic gripper during the task. The two-way ANOVA test revealed a statistically significant change in the angular motion for both the human involvement in the control ($F(1, 9) = 39.350$, $p < 0.001$) and the motion control type (position-velocity vs. velocity-velocity, $F(1, 9) = 8.202$, $p = 0.015$) variables. The one-way ANOVA test revealed a statistically significant change in the trajectory length across the conditions ($F(3, 27) = 12.994$, $p < 0.001$). Post hoc analysis with Bonferroni adjustments revealed a statistically significant difference between S+V vs. S+P ($p = 0.025$), S+V vs. T+V ($p = 0.007$), S+V vs. T+P ($p = 0.001$), S+P vs. T+V ($p = 0.039$), and S+P vs. T+P ($p = 0.005$).

Fig. 2d shows the perceived effectiveness for the four experimental conditions, asked using bipolar Likert-type nine-point scales. A Friedman test showed a statistically significant difference between the means of the four feedback conditions ($\chi^2(3) = 26.753$, $p < 0.001$, $\alpha = 0.05$). The Friedman test is the non-parametric equivalent of the more popular repeated-measures ANOVA. The latter is not appropriate here since the dependent variable was measured at the ordinal level. Post hoc analysis with Bonferroni adjustments revealed a statistically significant difference between S+V vs. T+V ($p < 0.001$), S+V vs. T+P ($p = 0.026$), S+P vs. T+V ($p < 0.001$), and S+P vs. T+P ($p = 0.044$).

IV. CONCLUSIONS

Results showed that, in all the considered metrics, the shared-control approach significantly outperformed the more classic teleoperation architecture. Moreover, all the subjects preferred the shared-control architecture with respect to teleoperation. This proves our hypothesis that shared-control can be a viable and very effective approach to improve currently-available teleoperation systems in remote manipulation tasks.

REFERENCES

- [1] E. Nuño, L. Basañez, and R. Ortega, “Passivity-based control for bilateral teleoperation: A tutorial,” vol. 47, no. 3, pp. 485–495, 2011.
- [2] J. Abbott, P. Marayong, and A. Okamura, “Haptic virtual fixtures for robot-assisted manipulation,” *Robotics Research*, pp. 49–64, 2007.
- [3] F. Abi-Farraj, T. Osa, N. Pedemonte, J. Peters, G. Neumann, and P. G. Robuffo, “A learning-based shared control architecture for interactive task execution,” in *IEEE Int. Conf. on Robotics and Automation*, 2017.
- [4] A. M. G. Esfahani, F. Abi-Farraj, P. R. Giordano, and R. Stolkin, “Human-in-the-loop optimisation: mixed initiative grasping for optimally facilitating post-grasp manipulative actions,” *arXiv:1707.08147*, 2017.
- [5] F. Farraj, N. Pedemonte, and P. Robuffo Giordano, “A visual-based shared control architecture for remote telemanipulation,” in *IEEE/RSJ Int. Conf. on Intelligent Robots and Systems*, 2016.